5-(4-(3-(substituted aryl/alkyl)-4-oxothiazolidin-2-yl)benzylidene)thiazolidine-2,4-dione molecules: Synthesis, Biological potential and *in silico* studies

Harsh Kumar
Maharshi Dayanand University
Davinder Kumar
Maharshi Dayanand University
Pradeep Kumar
Central University of Punjab
Suresh Thareja
Central University of Punjab
Minakshi Gupta Marwaha
Sat Priya College of Pharmacy
Uma Shankar
Central University of Punjab
Rakesh Kumar Marwaha (rkmarwaha.mdu@gmail.com)
Maharshi Dayanand University

Research Article

Keywords: Synthesis, Antimicrobial, Anticancer, Antioxidant, Characterization, Molecular docking, ADME

Posted Date: June 6th, 2022

DOI: https://doi.org/10.21203/rs.3.rs-1652194/v1

Abstract

Background: A novel series of thiazolidine-2,4-dione molecules was derived and their chemical structures were established using physiochemical parameters and spectral techniques (^{1}H-NMR, IR, MS etc.). The synthesized molecules were then evaluated for their antioxidant, anticancer and antimicrobial potential.

Results and discussion: Serial tube dilution method was employed to evaluate the antimicrobial potential against selected fungal and bacterial strains by taking fluconazole and cefadroxil as reference antifungal and antibacterial drugs respectively. 2,2-diphenyl-1-picrylhydrazyl (DPPH) free radical scavenging activity was used to assess the antioxidant potential of the synthesized analogues. The interactions of the derived thiazolidine-2,4-dione analogues with DNA gyrase and CDK8 enzymes were explored using molecular docking studies. Further, anticancer potential of the best docked molecules was assessed using MTT assay. The drug likeness was also evaluated by studying different ADME parameters of the synthesized analogues.

Conclusion: In antioxidant evaluation studies, the analogue **H5** with IC_{50} = 14.85 µg/mL was found to be the most active molecule. The antimicrobial evaluation outcomes suggested that the molecules **H5**, **H13**, **H15** and **H18** possessed moderate to promising activity against the selected species of microbial strains having MIC range 7.3 µM to 26.3 µM. The molecular docking studies revealed molecules **H18** (docking score = -4.07) and **H7** (docking score = -3.77) have reasonably fair docking score in the binding site of DNA gyrase in comparison to the reference drug. The molecules **H2** (docking score = -5.75) and **H10** (docking score = -5.41) having good score, exhibited decent interaction in the binding pocket of CDK8. The ADME studies revealed that all the compounds found to be drug like.

Introduction

The World Health Organization (WHO) reports indicates that the microbial drug resistance (MDR) caused due to continuous uses of presently available antibiotics and development of resistance against presently available anticancer drugs is the major concern for human life worldwide now a days [1, 2]. Clinical effectiveness of currently using antibiotics against most of the MDR strains, *viz*. vancomycin-resistant *enterococci* (VRE), multidrug resistant *staphylococcus aureus* (MRSA) etc. is shrinking constantly [3, 4]. This prompts the medicinal chemist/pharmacologist to explore their research to find the alternative antimicrobial drug therapies [5].

Cancer, one of the most terrible diseases and is the leading cause of death worldwide which accounts for approximately 17% of the total causalities. It has been charterized by uncontrolled and abnormal cells growth [6]. Inhibition of DNA replication and transcription to restrain the growth of tumor cells by currently used chemotherapeutic drugs is highly toxic [7], hence there is no ideal therapy currently available to cure cancer. This prompts medicinal chemists and researcher to find newer compounds having good antimicrobial and anticancer potential [2] with innovative mode of action and lesser toxic effect.

Thiazolidine-2,4-dione (TZD), a highly bioactive five membered heterocyclic ring system containing nitrogen and sulfur atoms along with two carbonyl groups, has generated special interest among the scientific community not only due to its diverse pharmacological potential but also due to various possibilities of chemical modification [8–9]. TZDs which are primarily known for their antidiabetic potential [10–12] also exhibited diverse therapeutic activities such as analgesic, anti-inflammatory [13–15], wound healing [16], antiproliferative [17–18], antimalarial [19], antitubercular [20–21], hypolipidemic [22], antiviral [23], antimicrobial [24–26] and antioxidant [27–28] etc.

Possible drug-receptor interaction can be determined using molecular docking studies which is a new rationale to drug design [29]. Drug designing techniques help in exploring new drug targets and molecules which exert specific action on human kind [30]. DNA (Deoxyribonucleic acid) gyrase, a member of topoisomerase II enzyme family, is an essential enzyme regulating the topological transitions of DNA by forming negative supercoils through strand breaking/resealing and DNA wrapping. It can be explored as important target for designing antimicrobial leads as its inhibition leads to DNA disruption and ultimately cell death [31].

The activity of human cyclin-dependent kinase (CDKs) is regulated through its association with CDK inhibitor proteins, their regulatory subunits (cyclins), by ubiquitin-mediated proteolysis and by their phosphorylation state and hence control the cell proliferation. The amplification and overexpression of CDK8 enzyme, a member of CDKs family, leads to development of tumors/cancer [9, 32]. The inhibition of CDK8 can provide an effective/ alternate approach for uncontrolled tumor/cancer growth.

The extreme surge in the cost of discovering new drug candidates, the drug discovery strategy has shifted to assess the comprehensive drug properties of the molecules under study at the earliest, for the clinical success of the drug candidates [33]. Pharmacokinetic parameters like absorption, distribution, metabolism and excretion (ADME) plays a vital role in dose defining, overall safety margins and dose intervals during drug development process [34]. Optimization of these parameters for a new chemical moiety having specific biological potential to be orally active is extremely important [5]. The molecules with poor ADME parameters may show unexpected toxicity, leading to withdrawal from the market and hence causing large financial losses [35]

Based on the literature survey and in continuation with our previous research efforts; in the present study, (4-oxothiazolidin-2-yl)thiazolidine-2,4-dione derivatives were synthesized and screened for antimicrobial, anticancer, antioxidant potential along with *in-silico* properties.

Results And Discussion

Chemistry

TZD derivatives (**H1-H19**) were synthesized by employing synthetic procedure as shown in Scheme 1. Initially, 2-chloroacetic acid was allowed to react with thiourea in presence of conc. HCl to get TZD (**INT-I**). Schiff's bases (**1–19**) were obtained by treating terephthalaldehyde and various substituted amines/anilines by taking acetic acid (glacial) as catalyst. Further compounds **1–19** were treated with thioglycolic acid using small quantity of zinc chloride as catalyst to obtain intermediates 4-(4-oxo-3-substitutedaryl/alkylthiazolidin-2-yl)benzaldehyde (**A1-A19**). Finally the reaction of **INT-I** with intermediates **A1-A19** yielded final derivatives 5-(-4-(3-(substituted aryl/alkyl)-4-oxothiazolidin-2-yl)benzylidene)thiazolidine-2,4-dione (**H1-H19**). The physicochemical parameters and spectral analysis of the synthesized analogues are summarized in Table 1. The molecular structures of the derived analogues (**H1-H19**) were established using different spectral techniques *viz.* FT-IR (KBr, cm^{-1}), ^{1}H-NMR (DMSO-d_6, 400 MHz, δ ppm), Mass spectra and elemental analysis. The presence of stretching bands at 3029 – 2885 cm^{-1}, 3199-2972cm^{-1}, 3498 – 3335 cm^{-1}, 1800 – 1687 cm^{-1}, 1556 – 1497 cm^{-1}, in IR spectrum, indicated the presence of C-H (aliphatic), C-H (aromatic), N-H, C = O, C = C (aromatic), respectively in the derived analogues. The presence of absorption bands around 1381 – 1232 cm^{-1}, 1696 – 1546 cm^{-1}, and 1196 – 1038 cm^{-1} in IR spectrum, corresponded to stretching vibrations of C-N, C = C (methylene) and C-C, respectively. The presence of absorption bands in the range of 847 – 801 cm^{-1} corresponds to C-H out of plane bending vibrations in the molecules. Appearance of bending absorption band at 680 – 618 cm^{-1} confirms the presence of C-S group. Compound **H4** possessed stretching absorption band of C-Cl around 761 cm^{-1}. Compounds **H12**, **H13** and **H19** displayed absorption bands at 1220 – 1176 cm^{-1} and 1437 – 1388 cm^{-1} of N-O and N = O groups respectively. The stretching band of O-CH_3 group in compounds **H15**, **H16** and **H17** was seen at 1033 – 1025 cm^{-1}. The aromatic protons present in the derived analogues were confirmed by the presence of multiplet signals between 6.68 and 7.95 δ ppm in the ^{1}H-NMR spectra. The appearance of singlet(s) between 12.46–12.61 δ ppm, 7.49–7.97 δ ppm, 5.22–6.95 δ ppm and confirmed the presence of -NH, -CH = and -CH of thiazolidin-4-one groups, respectively. In compound **H2** the presence of H of -NH_2 group was confirmed by presence of singlet (s) at 3.79 δ ppm. The presence of OCH_3 of Ar–OCH_3 in the compounds, **H15**, **H16** and **H17** was confirmed by appearance of singlet(s) at 2.88–3.79 δ ppm.

The presence of CH_3 (Ar-CH_3) in compounds **H8, H9** and **H10** is confirmed by the presence of singlet (s) at 2.12–2.73 δ ppm in ^{1}H-NMR spectra. In compound **H3** appearance of singlet at 9.61 δ ppm confirmed the presence of NH of Ar-NH. The existence of dodecyl group in compound **H5** is confirmed by the appearance of triplet at 0.90 δ ppm of CH_3, multiplet at 1.23–2.88 δ ppm of CH_2 and multiplet at 3.711 δ ppm of CH_2 adjacent to CH = N. The presence of furfuryl group in compound **H6** was due to presence of a doublet signal at 7.12 δ ppm corresponding to -CH of furan ring at 3rd position, singlet signal at 4.79 δ ppm due to -CH_2 group adjacent to furan ring, a triplet signal at 7.21 δ ppm due to -CH of furan ring at 4th position along with a doublet signal at 8.19 δ ppm due to -CH of furan ring adjacent to O (oxygen). The mass spectra of the derived analogues exhibited M^+, M^++1 and M^+-1 peaks.

Antimicrobial Screening

The *in vitro* antimicrobial evaluation of the synthesized analogues was carried out using serial tube dilution procedure (Table 2, Figs. 1, 2 and 3). The antifungal screening results indicated the compound **H5** to be moderately activity against *C. albicans* (MIC = 26.3 µM) and compound **H13** exhibited promising activity against *A. niger* (MIC = 7.3 µM) respectively. The results of antibacterial screening revealed that compound **H5** was moderately active against *S. aureus* (MIC = 13.2 µM). Antimicrobial screening results further revealed that compound **H18** possessed promising activity against *B. subtilis* and *S. typhi* (MIC = 7.8 µM) whereas the compound **H15** (MIC = 15.2 µM) has shown moderate activity against *E. coli* strain. The results of antifungal screening revealed that the derived analogues possess superior activity against both the selected strains of fungus *i.e., A. niger* and *C. albicans* while antibacterial screening results exhibited mild to moderate activity against the selected strains in comparison to cefadroxil as standard drug. So, these molecules can be viewed as lead structures for further development and optimization into potent antimicrobial agents.

Table 2
In vitro antimicrobial activity of the synthesized compounds

Comp.	Antimicrobial screening (MIC = µM)					
	SA	BS	EC	ST	CA	AN
H1	32.7	32.7	65.4	32.7	32.7	32.7
H2	77.8	38.9	38.9	38.9	38.9	38.9
H3	62.9	15.7	31.4	31.4	31.4	15.7
H4	30.0	15.0	60.0	15.0	30.0	30.0
H5	**13.2**	26.3	52.7	26.3	**26.3**	26.3
H6	32.3	32.3	32.3	32.3	32.3	32.3
H7	31.5	15.8	63.1	31.5	31.5	31.5
H8	63.1	31.5	63.1	31.5	31.5	31.5
H9	60.9	30.5	60.9	30.5	30.5	30.5
H10	60.9	15.2	60.9	30.5	30.5	30.5
H11	31.2	31.2	15.6	15.6	31.2	31.2
H12	54.2	27.1	54.2	13.5	27.1	27.1
H13	29.2	29.2	58.5	29.2	29.2	**7.3**
H14	27.1	27.1	54.1	27.1	27.1	13.5
H15	15.2	30.3	**15.2**	15.2	30.3	30.3
H16	30.3	30.3	60.6	30.3	30.3	15.2
H17	15.2	30.3	30.3	30.3	30.3	30.3
H18	15.6	**7.8**	31.2	**7.8**	31.2	7.8
H19	58.5	29.2	58.5	29.2	29.2	29.2
Cefadroxil	34.4	34.4	17.2	34.4	-	-
Fluconazole	-	-	-	-	40.8	40.8

SA: *Staphylococcus aureus*, BS: *Bacillus subtilis*, EC: *Escherichia coli*, ST: *Salmonella typhi;* CA: *Candida albicans*, AN: *Aspergillus niger*

Antioxidant evaluation

DPPH free radical scavenging assay was performed to assess the antioxidant potential of the newly synthesized derivatives using ascorbic acid as reference drug [36]. DPPH assay is among the most utilized methods used for assessing antioxidant potential of a compound which is based on chain-breaking mechanism. DPPH is a stable free radical which can be transformed into a constant diamagnetic molecule by accepting a hydrogen or an electron radical from the antioxidant compound [37]. The DPPH solution (methanolic) exhibit a strong absorption band at 517 nm. As DPPH radical reacts with the antioxidant/ reducing agent, a new bond is generated which leads to decreases in the color intensity of the solution. As the strength of antioxidants in the solution is increased, the DPPH radical takes up a greater number of electrons, leading to loss in the color intensity of the solution from purple to pale yellow which is monitored spectrophotometrically at 517 nm [38]. The IC_{50} value (µg/mL) and % inhibition for all the synthesized molecules was calculated. The antioxidant screening assay revealed that the derived molecules were more potent than the reference drug itself. Further, the antioxidant screening showed compound **H5** (IC50 = 14.85 µg/mL) be the most potent. Antioxidant evaluation results are depicted in Table 3 and Fig. 4.

Table 3
In vitro antioxidant activity of the synthesized compounds

Comp.	% Inhibition				Antioxidant activity (IC_{50} = µg/ml)
	25 µg/mL	50 µg/mL	75 µg/mL	100 µg/mL	
H1	21.18	38.03	50.98	63.92	29.58
H2	36.86	43.92	49.80	56.47	29.99
H3	27.45	43.13	56.86	62.74	27.04
H4	15.68	36.47	45.88	56.07	33.78
H5	43.92	56.08	67.84	76.08	**14.85**
H6	40.78	52.94	61.57	72.16	18.32
H7	29.02	48.63	62.35	68.24	23.43
H8	21.18	40.78	55.69	63.53	28.31
H9	36.86	42.35	54.90	72.94	23.53
H10	27.84	48.24	60.39	66.27	24.46
H11	32.55	43.14	51.76	59.61	28.60
H12	23.53	47.84	57.25	67.45	25.69
H13	21.96	32.16	48.24	60.39	32.09
H14	9.41	21.96	40.00	47.45	35.31
H15	12.94	29.80	44.71	50.98	36.93
H16	32.16	41.96	48.24	64.31	28.24
H17	22.35	32.16	52.55	58.82	31.57
H18	9.41	26.27	36.86	52.55	38.37
H19	36.47	48.63	60.39	65.49	22.22
Ascorbic Acid	16.08	30.20	40.39	48.62	40

Molecular Docking Results

Among different *in-silico* drug designing tools used now a days, molecular docking is viewed as most prominent component of modern medicinal chemistry as it uses three-dimensional structural information to identify the possible biological targets [39]. The DNA gyrase (antimicrobial) and CDK8 (anticancer) enzymes were selected as biological target for molecular docking studies in present study. The enzyme DNA gyrase, which belongs to the family of topoisomerases class II, is responsible for controlling the topology of DNA in cells and comprises of two genes *i.e.* GyrA (DNA gyrase subunit A) and GyrB (DNA gyrase subunit B) [40].

In the cell replication process, DNA topology is maintained by DNA gyrase during supercoiling of DNA through its coupling with ATP (Adenosine triphosphate) hydrolyzed by the GyrB subunit. Therefore, the inhibition of DNA gyrase enzyme leads to disruption of DNA synthesis in bacterial species resulting in death of bacterial cells [41].

CDK-8 is a heterodimeric kinase protein helps in transcription and also regulate the progression of cell cycle along with other functions of RNA polymerase II. The regulatory subunit cyclin provides additional sequences of enzymatic activity of CDKs. CDKs (1, 4, 5, 7, 8, 9 and 11) possessed a two-lobed structure having C-terminal composed of α-helices and N-terminal consists of beta sheets [29, 42]. CDK-8 modulates several transcriptional factors *i.e.* p53, Notch, Wnt/β-catenin pathway and TGF-β which helps in oncogenic control. The over expression of CDK8/CDK19 leads to prostate cancer and its inhibition will provide an impact in regulating the tumor growth and can be an effective drug target for prostate cancer treatment [43].

The current study was carried out using Drug Discovery Software - Schrödinger 2020 (https://www.schrodinger.com).GLIDE module of Schrödinger 2020-4 (Maestro version *12.5*) software was used to carry the docking procedure [44]. Molecular docking technique was used to evaluate the binding affinity of the ligands with the ATP binding pocket of DNA gyrase enzyme and is computed in term of negative energy. All the synthesized molecules were docked in the active site of the microproteins (PDB: 3U2D) of *S. aureus* GyrB ATPase domain (co-crystallized

with 08B ligand) and human cyclin-dependent kinase CDK-8 (PDB: 5-FGK) enzyme (co-crystallized with 5XG ligand). The binding affinity of compounds was computed in terms of docking score obtained from GLIDE module and compared with the standard drugs (Table 4).

The binding affinity of the analogues with the receptor pocket was depicted by their binding energy and was calculated as negative energy *i.e.* lesser the binding energy, stronger is the binding affinity. The term Docking scores was used to show the interaction energy in terms of numerical value which is statistically evaluated function for analysing the results. Various visualization tools were employed for visualization of 3D poses of the ligand-receptor interaction [45].

Table 4
In silico docking score of the synthesized compounds with 3U2D protein and 5 FGK protein.

Comp.	Docking Score (3U2D)	Docking Score (5FGK)
H1	-3.202	-4.362
H2	-3.55	**-5.748**
H3	-3.387	-4.514
H4	-2.849	-5.046
H5	-3.745	-3.246
H6	-3.235	-4.088
H7	**-3.774**	-4.609
H8	-3.254	-3.835
H9	-2.943	-4.5
H10	-2.315	-5.417
H11	-3.345	-5.302
H12	-2.877	-3.147
H13	-3.566	-4.36
H14	-3.155	-3.853
H15	-2.863	-4.233
H16	-3.118	-4.283
H17	-3.589	-4.007
H18	**-4.07**	-4.135
H19	-2.918	-2.309
Ofloxacin	-5.107	—
5-Fluorouracil	—	-4.015

Molecular docking study indicated that the derived analogues exhibited comparable interaction with the important amino acids of the DNA gyrase protein. The best-fitted compounds **H5** and **H7** exhibited the good docking scores of -4.07 and − 3.77, respectively when compared with marketed drug ofloxacin (docking score = -5.107) in the binding pocket of ATP (Table 5). The binding mode and the ligand interaction diagram of most active compounds **H5**, **H7** and standard drug ofloxacin in the active site of *S. aureus* GyrB ATPase domain as shown in Table 5, Figs. 5, 6 and 7.

Table 5

Docking score and binding energy of compounds **H18** and **H7** with standard drug ofloxacin

Compound	Docking Score	Interacting Residues
H18	-4.07	PRO87, ILE86, GLY85, ARG84, GLY83, ASP81, THR173, ILE175, GLU 58, ASP57, SER55, ASN54, ILE51, LEU103, ILE102
H7	-3.774	PRO87, ILE86, GLY85, ARG84, GLY83, ASP81, VAL79, THR173, ILE175, GLU 58, ASP57, SER55, ASN54, ILE51, LEU103, ILE102
Ofloxacin	-5.107	PRO87, ILE86, GLY85, ARG84, GLY83, ASP81, VAL131, SER129, SER128, LEU103, ILE102, THR173, ILE175, GLU58, SER55, ASN54, ILE51

In case of CDK8 protein co-crystallized with 5XG ligand, most active compounds **H2** and **H10** exhibited the good interaction within the ATP pocket with docking score of -5.75 and – 5.41, respectively and has better docking score than standard drug 5-FU (-4.02). The ligand interaction diagram and binding mode of the standard drug and most active compounds were expressed in (Table 6, Figs. 8, 9 and 10).

Table 6

Docking score and binding energy of compounds **H2** and **H10** with standard drug 5-fluorouracil

Compound	Docking Score	Interacting Residues
H2	-5.75	VAL27, GLY28, TYR32, VAL35, ALA50, ILE79, PHE97, ASP98, TYR99, ALA100, LYS153, ALA155, ASN156, LEU158, ASP173, ALA172, ARG356, DMS402
H10	-5.41	VAL27, GLY28, TYR32, VAL35, ALA50, LYS52, ILE79, PHE97, ASP98, TYR99, ALA100, LYS153, ALA155, ASN156, LEU158, ASP173, ALA172, ARG356, DMS402
5-FU	-4.02	VAL27, VAL35, ALA50, ILE79, PHE97, ASP98, TYR99, ALA100, LEU158, ARG356, DMS402

ADME results

The synthesized derivatives (**H1-H19**) were submitted to QikProp module of Schrödinger software 2020-4 (Maestro version *12.5*) for the calculation of ADME parameters [46]. The results of ADME studies were promising and within the defined range of Qikprop module. Various physically relevant and pharmacologically significant parameters of the synthesized derivatives were studied and found to be within Lipinski's rule of five range. The parameters studied included Predicted skin permeability (QPlogKp = -8.0 to-1.0), Molecular weight of the molecule (mol. MW = < 500), human oral absorption (1, 2 or 3), Predicted blood /brain partition coefficient (QPlogBB = -3.0 to -1.2), Predicted gas/water partition coefficient (QPlogPw = 4.0 to -45.0), Predicted water /octanol partition coefficient (QPlogPo/w = -2.0 to -6.5), Percent human oral absorption (0 to 100), accept HB (2.0 to -20.0), donor HB (0.0 to -6.0) and results revealed these molecules as appropriate drug candidates. The ADME studies results are summarized in the Table 7.

Table 7
ADME parameters of synthesized compounds

Comp.	ADME parameters										
	Mol MW	Rule of Five	QPlogPo/w	Human Oral Absorption	Volume	% Human Oral Absorption	QPlogP$_w$	QPlogK$_p$	QPlogBB	Donor HB	Accept HB
H1	382.451	0	2.938	3	1083.522	88.762	11.638	-3.26	-0.864	1.0	6.5
H2	321.318	0	1.017	3	895.076	67.663	13.451	-4.786	-1.339	3.0	6.5
H3	397.466	0	2.648	3	1071.33	88.868	12.756	-2.99	-0.716	2.0	7.0
H4	416.896	0	3.378	3	1121.417	91.86	11.479	-3.3	− .0.685	1.0	6.5
H5	474.675	1	5.179	1	1560.744	86.143	11.023	-2.583	-1.72	1.0	6.5
H6	386.413	0	2.075	3	1031.416	83.314	11.847	-3.425	-0.85	1.0	7.0
H7	396.478	0	3.264	3	1137.026	92.005	11.244	-3.312	-0.77	1.0	6.5
H8	396.478	0	3.238	3	1143.692	90.455	11.336	-3.466	-0.917	1.0	6.5
H9	410.505	0	3.563	3	1194.624	93.175	11.135	-3.488	-0.862	1.0	6.5
H10	410.505	0	3.406	3	1148.371	94.491	11.07	-3.17	-0.599	1.0	6.5
H11	400.442	0	3.093	3	1092.485	89.859	11.429	-3.349	-0.752	1.0	6.5
H12	461.347	0	3.495	3	1136.077	91.969	11.403	-3.439	-0.723	1.0	6.5
H13	427.449	0	2.262	3	1154.785	69.373	12.711	-5.044	-1.858	1.0	7.5
H14	461.894	0	2.863	3	1181.117	77.794	12.25	-4.654	-1.299	1.0	7.5
H15	412.477	0	3.051	3	1160.063	89.311	11.907	-3.34	-0.915	1.0	7.25
H16	412.477	0	3.027	3	1123.234	93.623	11.593	-2.874	-0.549	1.0	7.25
H17	412.477	0	3.033	3	1159.589	89.485	11.807	-3.362	-0.926	1.0	7.25
H18	400.442	0	3.174	3	1101.044	90.007	11.432	-3.408	-0.777	1.0	6.5
H19	427.449	0	2.238	3	1158.399	68.166	12.751	-5.165	-1.94	1.0	7.5

Anticancer potential

Anticancer potential of three synthesized derivatives having best docking score *viz.* **H2**, **H10** and **H11** were tested for their *in vitro* anticancer potential against prostate cancer cell line (DU-145) using MTT assay. The results of anticancer evaluation revealed that all screened derivatives possess mild/negligible potential (Fig. 11) when compared with standard drug 5-FU (IC_{50} = 5.2 µM).

Structure activity relationship (SAR)

From the results of antimicrobial, anticancer and antioxidant evaluation studies, the following SAR can be expressed (Fig. 12):

- Various substituent(s) present on aliphatic/aromatic amines used for the synthesis of the final analogues of 5-(-4-(3-(substituted aryl/alkyl)-4-oxothiazolidin-2-yl)benzylidene)thiazolidine-2,4-dione (**H1-H19**), have vital impact on the antimicrobial, anticancer and antioxidant potential of the synthesized molecules.
- Presence of electron donating group (-OCH_3) at *ortho* position in molecule **H15** enhanced antibacterial activity against *E. coli.*
- Substitution of nitro (-NO_2) group at *meta* position (electron withdrawing) in molecule **H13** enhanced antifungal activity against *A. niger*.
- Presence of (-F) group (electron withdrawing) at *para* position in molecule **H18** enhanced the antibacterial activity against *S. typhi* and *B. subtilis* whereas substitution of aliphatic group dodecyl in the derived molecule **H5**, enhanced the antioxidant activity and also exhibited better antimicrobial potential against *S. aureus* and *C. albicans*.
- Presence of amino group in molecule **H2** exhibited good anticancer activity.

Conclusion

A series of thiazolidine-2,4-dione clubbed with thiazolidine-4-one molecules was synthesized and then screened for its antimicrobial, anticancer and antioxidant potential. The molecules **H5**, **H13**, **H15** and **H18** exhibited moderate to good antimicrobial activity against various selected strains of microbial species with MIC ranging from 7.3 µM to 26.3 µM in antimicrobial screening assay. In antioxidant evaluation assay, the compound **H5** was found to be the best antioxidant molecule among the synthesized series with IC_{50} value of 14.85 µg/mL. The outcome of molecular docking studies indicated molecules **H18** (dock score = -4.07) and **H7** (dock score = -3.77), possess fairly good interaction in the DNA gyrase binding pocket. Molecules **H2** (dock score = -5.75) and **H10** (dock score = -5.41) with good docking score, exhibited decent interaction in the binding pocket of CDK and ADME studies revealed that all the compounds found to be drug like to be orally active as all the parameters of the compounds was found within Lipinski's rule of five. These derivatives can be used as lead structures for further modification/optimization into more potent antimicrobial, anticancer and antioxidant drug molecules with least toxicity.

Experimental

The chemicals used in the synthetic work were either of AR or LR grade purchased from different vendors and were used as such without any further purification.

The melting point (m.p.) of the synthesized compounds was determined by using Stuart scientific SMP3 apparatus on open glass capillaries and reported uncorrected. The progress of every synthetic step was monitored using TLC (Thin layer chromatography) on precoated silica gel G plates. Bruker 12060280 (Software: OPUS 7.2.139.1294) spectrophotometer was used for recording infrared (IR, KBr, cm^{-1}) by taking KBr pellets. ^1H spectral determination was recorded on Bruker Avance III 400 NMR spectrometer by taking appropriate deuterated solvents and are expressed in parts per million (δ, ppm) downfield from internal standard tetramethylsilane. Waters Micromass Q-ToF Micro instrument was used for recording the mass spectra of the synthesized derivatives. Elemental analysis was recorded using CHNS analyzer.

Synthetic steps of Scheme 1:

Step 1: Synthesis of thiazolidin-2,4-dione TZD **(INT-I)**:

Aqueous solution of thiourea (0.06 mol in 15 mL of water) was added dropwise to the aqueous solution of chloroacetic acid (0.06 mol in 15 mL of water) and stirred constantly till the formation of white precipitates. 6 mL of conc. HCl was then added dropwise in the above mixture and then refluxing was carried for 10 h. Fine needle shaped crystals of TZD (**INT-I**) were formed on cooling which were filtered, dried and recrystallized from methanol [27].

Step 2: Synthesis of (E)-4-((substitutedaryl/alkylimino)methyl)benzaldehyde **(1–19)**:

To a solution of terephthalaldehyde (0.01 mol) in ethanol (25 mL), various substituted amines/anilines in equimolar amount were added using acetic acid (glacial) as catalyst and refluxing was done for 6–15 h. The reaction mixture was then allowed to cool to obtain solid which was further recrystallized from methanol to give intermediate Schiff's bases **(1–19)** [29].

Step 3: Synthesis of 4-(4-oxo-3-substitutedaryl/alkylthiazolidin-2-yl)benzaldehyde **(A1-A19)**:

The solution of 0.015 mol of thioglycolic acid in 20 ml of N,N-dimethylformamide (DMF) was added dropwise with constant stirring to the (0.01 mol) solution of Schiff's base (**1–19**) prepared in DMF. A pinch of anhydrous $ZnCl_2$ was added into the reaction mixture followed by refluxing for about 6–8 h. The rection mixture was then cooled and poured on to crushed ice. The solid so obtained was filtered and washed with cold distilled water. The product after drying was recrystallized from methanol to obtain intermediate derivatives (**A1-A19**) [47].

Step 4: Synthesis of various title compounds **(H1-H19)**:

To the solution of **INT-I** (0.01 mol) in DMF (10 mL), compounds **A1-A19** in DMF were added followed by addition of 3 mL of piperidine (0.0188 mol). the contents of the flask was then stirred and refluxed for next 12–24 h. on completion of reaction; the reaction mixture was then poured on ice followed by acidification with acetic acid (glacial) to obtain final crude compounds 5-(-4-(3-(substitutedaryl/alkyl)-4-oxothiazolidin-2-yl)benzylidene) thiazolidine-2,4-dione (**H1-H19**). The product after drying was recrystallized from methanol to obtain final pure compounds.

In vitro **antimicrobial evaluation**

The synthesized molecules were screened for their antimicrobial potential by serial tube dilution method [48] by comparing with marketed antibiotics; cefadroxil (antibacterial screening) fluconazole (antifungal screening). The evaluation was carried out using both Gram -ve {MTCC-3231 (*S. typhi*), MTCC-443 (*E. coli*)} and Gram + ve {MTCC-441 (*B. subtilis*), MTCC-3160 (*S. aureus*)} bacterial strains. The antifungal screening study was assessed using two fungal strains {MTCC-281 (*A. niger*), MTCC-227 (*C. albicans*)}. The antimicrobial screening was carried out by using Sabouraud dextrose broth I.P. (for fungi) or Nutrient broth double strength I.P. (for bacteria) [49] nutrient media. Dimethyl sulfoxide was

used as diluting mediun for the preparation of stock solutions of the reference and test molecules along with a control set of same dilutions. Incubation the samples at 37 ± 1°C (24 h) for bacteria, at 37 ± 1°C (48 h) for *C. albicans* and at 25 ± 1°C (7 days) for *A. niger*, respectively. Results were recorded as MIC for the tested molecules that exhibited no observable growth of microorganisms in the test tube at lowest possible concentration.

In vitro **antioxidant assay**

The antioxidant potential of synthesized thiazolidine-2,4-dione molecules was analyzed using DPPH free radical scavenging assay [50]. Synthesized compounds were diluted to 25 µg/mL, 50 µg/mL, 75 µg/mL and 100 µg/mL concentration with methanol and kept in different test tube. To these test tube equal quantity of 0.0039% DPPH in methanol was added followed by vigorous shaking. The test tubes containing above mixture was then wrapped with silver foil paper and kept in dark room for 30 minutes. Finally, UV-visible double beam spectrophotometer was used to measure the absorbance of the mixtures at 517 nm. Mean IC_{50} value of at least three observations is presented in the data.

Molecular Docking Study

The target proteins *i.e. S. aureus* GyrB ATPase (co-crystallized with 08B ligand) and human cyclin-dependent kinase CDK-8 (PDB: 5-FGK) enzyme (co-crystallized with 5XG ligand) identified from literature were retrieved from Protein Data Bank (http://www.rcsb.org/pdb/home/home.do). ATPase is an outstanding target against *S. aureus* strain [51] for their antimicrobial activity and Human CDK8 regulates transcription of RNA for their anticancer potential to dock derived thiazolidine-2,4-dione analogues. GLIDE Module was used to calculate the docking score by creating the active site grid and interactions of ligands/molecules with vital amino acids of ATP [52].

In vitro **anticancer screening**

The anticancer screening was done using MTT (3-(4,5-dimethylthiazol-2-yl)-2,5-diphenyltetrazolium bromide) assay. Firstly, cells of DU-145 were seeded (5×10^3 cells/well) at clear 96-well plates. After 24 h, synthesized derivatives in concentration of 1 µM, 3 µM, 10 µM, 30 µM, 90 µM, 150 µM, 270 µM, 350 µM, 500 µM, 700 µM were added in each well to expose the cell lines for further 24 h. The medium *i.e.* DMSO was added to the control wells. After completion of incubation period the cells were washed with sterile phosphate buffer and 100 µL of MTT solution in each well was added and further incubation was done for 4 h. MTT solution was then removed by inverting the well plate and 150 µL of DMSO was then added to dissolve insoluble formazan crystals. The optical density at 570 nm was determined spectrophotometrically. The anticancer potential was expressed as the relative cell viability (%) relative to the untreated control cells [53].

Abbreviations

TZD: Thiazolidin-2,4-dione

MIC: Minimum inhibitory concentration

FT-IR: Fourier transform infrared

IC_{50}: Half maximal inhibitory concentration

µM: micro mole

CDK: Cyclin dependent kinase

GyrA: DNA gyrase subunit A

GyrB: DNA gyrase subunit B

TLC: Thin layer chromatography

5-FU: 5-Fluorouracil

PDB: protein data bank

MTT: (3-(4, 5-dimethylthiazolyl-2)-2, 5-diphenyltetrazolium bromide)

DNA: Deoxyribonucleic acid

DMS: Dimethyl suberimidate

TYR: tyrosine

ILE: Isoleucine

VAL: Valine

GLY: Glycine

PHE: Phenylalanine

ASP: Aspartic acid

ASN: Asparagine

LYS: Lysine

LEU: Leucine

H-NMR: Proton nuclear magnetic resonance

MS: Mass spectrometry

ADME: absorption, distribution, metabolism and excretion

DPPH: 2,2-Diphenyl-1-picrylhydrazyl

ATP: Adenosine triphosphate

MRSA: Multidrug resistant *staphylococcus aureus*

VRE: Vancomycin-resistant *enterococci*

Declarations

Availability of data and materials: All data generated or analyzed during this study are included in this published article.

Ethical Approval and consent to participate: Not applicable.

Competing interest: The authors declares that they have no competing interest.

Funding- Not applicable.

Author's Contributions

HK, RKM, DK: Designed, synthesized and performed the antimicrobial and antioxidant activities; PK, MGM, ST: performed the molecular docking, spectral analysis and helped in the structure interpretation of the synthesized compounds; US: performed the anticancer activity of most active docked molecules. All authors have carefully read the manuscript and approved it.

Acknowledgements

The authors are thankful to Head, Department of Pharmaceutical Sciences, Maharshi Dayanand University, Rohtak, for providing necessary facilities to carry out this research work.

References

1. Althagafi I, Farghaly TA, Abbas EMH, Harras MF. Benzosuberone as Precursor for Synthesis of Antimicrobial Agents: Synthesis, Antimicrobial Activity, and Molecular Docking. Polycycl Aromat Compd. 2021;41(8):1646-66.

2. Kumar H, Kumar P, Narasimhan B, Ramasamy K, Mani V, Mishra RK, et al. Synthesis, in vitro antimicrobial, antiproliferative, and QSAR studies of *N*-(substituted phenyl)-2/4-(1*H*-indol-3-ylazo)-benzamides. Med Chem Res. 2013;22:1957-71.

3. Zamperini C, Maccari G, Deodato D, Pasero C, D'Agostino I, Orofino F, et al. Identification, synthesis and biological activity of alkyl-guanidine oligomers as potent antibacterial agents. Sci Rep. 2017;7:8251.

4. Keche AP, Hatnapure GD, Tale RH, Rodge AH, Birajdar SS, Kamble VM. Novel pyrimidine derivatives with aryl urea, thiourea and sulfonamide moieties: synthesis, anti-infammatory and antimicrobial evaluation. Bioorg Med Chem Lett. 2012;22(10):3445–48.

5. Sharma D, Kumar S, Narasimhan B, Ramasamy K, Lim SM, Shah SAA, et al. 4-(4-Bromophenyl)-thiazol-2-amine derivatives: synthesis, biological activity and molecular docking study with ADME profile. BMC Chem. 2019;13:60.

6. Sharma D, Kumar S, Narasimhan B, Ramasamy K, Lim SM, Shah SAA, et al. Synthesis, molecular modelling and biological significance of N-(4-(4-bromophenyl)thiazol-2-yl) -2-chloroacetamide derivatives as prospective antimicrobial and antiproliferative agents. BMC Chem. 2019;13:46.

7. Tahlan S, Kumar S, Ramasamy K, Lim SM, Ali Shah SA, Vasudevan M, et al. In-silico molecular design of heterocyclic benzimidazole scaffolds as prospective anticancer agents. BMC Chem. 2019;13:90.

8. Trotsko N, Kosikowska U, Paneth A, Plech T, Malm A, Wujec M. Synthesis and Antibacterial Activity of New Thiazolidine-2,4-dione-Based Chlorophenylthiosemicarbazone Hybrids. Molecules. 2018;23(5):1023.

9. Parekh NM, Juddhawala KV, Rawal BM. Antimicrobial activity of thiazolyl benzene sulfonamide-condensed 2,4-thiazolidinediones derivatives. Med Chem Res. 2012;22:2737–45.

10. Jiang B, Luo J, Guo S, Wang L. Discovery of 5-(3-bromo-2-(2,3-dibromo-4,5-dimethoxybenzyl)-4,5-dimethoxybenzylidene)thiazolidine-2,4-dione as a novel potent protein tyrosine phosphatase 1B inhibitor with antidiabetic properties. Bioorg Chem. 2021;108:104648.

11. Fettach S, Thari FZ, Hafidi Z, Karrouchi K, Bouathmany K, Cherrah Y, et al. Biological, toxicological and molecular docking evaluations of isoxazoline-thiazolidine-2,4-dione analogues as new class of anti-hyperglycemic agents. J Biomol Struct Dyn. 2021; https://doi.org/10.1080/07391102.2021.2017348.

12. Mohd Siddique MU, Thakur A, Shilkar D, Yasmin S, Halakova D, Kovacikova L, et al. Non-Carboxylic Acid Inhibitors of Aldose Reductase Based on N-Substituted Thiazolidinedione Derivatives. Eur J Med Chem. 2021;223:113630.

13. Abdellatif KRA, Fadaly WAA, Kamel GM, Elshaier, YAMM, El-Magd MA. Design, synthesis, modeling studies and biological evaluation of thiazolidine derivatives containing pyrazole core as potential anti-diabetic PPAR-γ agonists and anti-inflammatory COX-2 selective inhibitors. Bioorg Chem. 2019;82:86-99.

14. Elkamhawy A, Kim NY, Hassan AHE. Park JE, Paik S, Yang JE, et al. Thiazolidine-2,4-dione-based irreversible allosteric IKK-β kinase inhibitors: Optimization into in vivo active anti-inflammatory agents. Eur J Med Chem. 2020;188:111955.

15. Asati V, Bajaj S, Mahapatra DK, Bharti SK. Molecular Modeling Studies of Some Thiazolidine-2,4-Dione Derivatives as 15-PGDH Inhibitors. Med Chem Res. 2015;25(1): 94-108.

16. Yu I, Choi D, Lee HK, Cho H. Synthesis and Biological Evaluation of New Benzylidenethiazolidine-2,4-Dione Derivatives as 15-Hydroxyprostaglandin Dehydrogenase Inhibitors to Control the Intracellular Levels of Prostaglandin E2 for Wound Healing. Biotechnol Bioprocess Eng. 2019;24(3):464-75.

17. Ibrahim HS, Abdelsalam M, Zeyn Y, Zessin M, Mustafa AHM, Fischer MA, et al. Synthesis, molecular docking and biological characterization of pyrazine linked 2-aminobenzamides as new class i selective histone deacetylase (hdac) inhibitors with anti-leukemic activity. Int J Mol Sci. 2022;23:369.

18. El-Kashef H, Badr G, Abo El-Maali N, Sayed D, Melnyk P, Lebegue N, et al. Synthesis of a novel series of (Z)-3,5-disubstituted thiazolidine-2,4-diones as promising anti-breast cancer agents. Bioorg Chem. 2020;96:103569.

19. Sharma RK, Younis Y, Mugumbate G, Njoroge M, Gut J, Rosenthal PJ. et al. Synthesis and structure activity-relationship studies of thiazolidinediones as antiplasmodial inhibitors of the Plasmodium falciparum cysteine protease falcipain-2. Eur J Med Chem. 2015;90:507–18.

20. Ratnaparkhi H, Thakar S, Bansode D. An overview of chemistry and antitubercular activity of thiazolidinediones. Sch Acad J Pharm. 2020;9(1):23-31.

21. Trotsko N, Golus J, Kazimierczak P, Paneth A, Przekora A, Ginalska G, et al. Synthesis and antimycobacterial activity of thiazolidine-2,4-dione based derivatives with halogenbenzohydrazones and pyridinecarbohydrazones substituents. Eur J Med Chem. 2020;189:112045.

22. Mohammed Iqbal AK, Khan AY, Kalashetti MB, Belavagi NS, Gong YD, Khazi IAM. Synthesis, hypoglycemic and hypolipidemic activities of novel thiazolidinedione derivatives containing thiazole/triazole/oxadiazole ring. Eur J Med Chem. 2012;53:308-15.

23. Bahare RS, Ganguly S, Choowongkomon K, Seetaha S. Synthesis, HIV-1 RT inhibitory, antibacterial, antifungal and binding mode studies of some novel N-substituted 5-benzylidine-2, 4-thiazolidinediones. DARU J Pharm Sci. 2015:23(1):6.

24. Aziz HA, El-Saghier AMM, Badr M, Abuo-Rahma GEDA, Shoman ME. Thiazolidine-2,4-dione-linked ciprofloxacin derivatives with broad-spectrum antibacterial, MRSA and topoisomerase inhibitory activities. Mol Divers. 2021; https://doi.org/10.1007/s11030-021-10302-7.

25. Alegaon SG, Venkatasubramanian U , Alagawadi KR, Kumar D, Kavalapure RS, Ranade SD, et al. Synthesis, molecular docking and ADME studies of thiazole-thiazolidinedione hybrids as antimicrobial agents. J Biomol Struct Dyn. 2021; https://doi.org/10.1080/07391102.2021.1880479.

26. Moorthy P, Ekambaram SP, Perumal SS. Synthesis, characterization and antimicrobial evaluation of imidazolyl thiazolidinedione derivatives. Arab J Chem. 2019;12(3):413–19.

27. Kumar H, Deep A, Marwaha RK. Design, synthesis, in silico studies and biological evaluation of 5-((E)-4-((E)-(substituted aryl/alkyl)methyl)benzylidene)thiazolidine-2,4-dione derivatives. BMC Chem. 2020;14:25.

28. Sameeh MY, Khowdiary MM, Nassar HS, Abdelall MM, Alderhami SA, Elhenawy AA. Discovery potent of thiazolidinedione derivatives as antioxidant,
α-amylase inhibitor and antidiabetic agent. Biomedicines. 2022;10:24.

29. Kumar S, Lim SM, Ramasamy K, Vasudevan M, Ali Shah SA, Selvaraj M, et al. Synthesis, molecular docking and biological evaluation of bis-pyrimidine Schiff base derivatives. Chem Cent J. 2017;11:89.

30. Kumar S, Kaushik A, Narasimhan B, Ali Shah SA, Lim SM, Ramasamy K, et al. Molecular docking, synthesis and biological significance of pyrimidine analogues as prospective antimicrobial and antiproliferative agents. BMC Chem. 2019;13:85.

31. Perumal P, Pandey VP, Parasuraman P. Docking studies on some novel piperidine analogues against DNA gyrase enzyme. Inventi Rapid Molecular Modeling. 2014;1:1-4.

32. Koehler MFT, Bergeron P, Blackwood EM, Bowman K, Clark KR, Firestein R, et al. Development of a potent, specific CDK8 kinase inhibitor which phenocopies CDK8/19 knockout cells. ACS Med Chem Lett. 2016;7:223–28.

33. Wang J, Urban L, Bojanic D. Maximising use of in vitro ADMET tools to predict in vivo bioavailability and safety. Expert Opin Drug Metab Toxicol. 2007;3(5):641-65.

34. Gleeson MP, Hersey A, Hannongbua S. In-Silico ADME Models: A general assessment of their utility in drug discovery applications. Curr Top Med Chem. 2011;11(4):358-81.

35. Li AP. Screening for human ADME/Tox drug properties in drug discovery. Res Focus. 2001;6(7):357–66.

36. Nyaki HY, Mahmoodi NO. Synthesis and characterization of derivatives including thiazolidine-2,4-dione/1-H- imidazole and evaluation of antimicrobial, antioxidant, and cytotoxic properties of new synthetic heterocyclic compounds. Res Chem Intermed. 2021;47:4129-55.

37. Mardani-Ghahfarokhi A, Farhoosh R. Antioxidant activity and mechanism of inhibitory action of gentisic and α-resorcylic acids. Sci Rep. 2020;10:19487.

38. Redon J, Oliva MR, Tormos C, Giner V, Chaves J, Iradi A, et al. Antioxidant activities and oxidative stress by products in human hypertension. J Hypertens. 2003;1(1):1096-109.

39. Ferreira LG, Dos Santos RN, Oliva G, Andricopulo AD. Molecular docking and structure-based drug design strategies. Molecules. 2015;22;20(7):13384-421.

40. Wang JC. Untangling the double helix: DNA entanglement and the action of the DNA topoisomerases. Cold Spring Harbor, New York, 2019.

41. Maxwell A, Lawson DM. The ATP binding site of type II topoisomerases as a target for antibacterial drugs. Curr Top Med Chem. 2003;3:283–303.

42. Kalra S, Joshi G, Munshi A, Kumar R. Structural insights of cyclin dependent kinases: implications in design of selective inhibitors. Eur J Med Chem. 2017;142:424–58.

43. Offermann A, Joerg V, Becker F, Roesch MC, Kang D, Lemster A-L, et al. Inhibition of Cyclin-Dependent Kinase 8/Cyclin-Dependent Kinase 19 Suppresses Its Pro-Oncogenic Effects in Prostate Cancer. Am J Pathol. 2022;192:813-23.

44. Glide, Schrödinger, LLC, New York, NY, 2020

45. Bassyouni F, El Hefnawi M, El Rashed A, Rehim MA. Molecular modeling and biological activities of new potent antimicrobial, anti-inflammatory and anti-nociceptive of 5-nitro indoline-2-one derivatives. Drug Des. 2017;6(2):1-6.

46. QikProp, Schrödinger, LLC, New York, NY, 2020

47. Deep A, Jain S, Sharma PC, Mittal SK, Phogat P, Malhotra M. Synthesis, characterization and antimicrobial evaluation of 2,5-disubstituted-4-thiazolidinone derivatives. Arab J Chem. 2014;7:287-91.

48. Cappuccino JC, Sherman N. Microbiology-a laboratory manual. California: Addison Wesley; 1999. p 263.

49. Pharmacopoeia of India, vol.-I. New Delhi: Controller of publication, ministry of health department, Govt. of India; 2007. p. 37.

50. Koppireddi S, Komsani JR, Avula S, Pombala S, Vasamsetti S, Kotamraju S, et al. Novel 2-(2,4-dioxo-1,3-thiazolidin-5-yl)acetamides as antioxidant and/or anti-inflammatory compounds. Eur J Med Chem. 2013;66:305-13.

51. Jas MJS, Marimuthu G, Prithivirajan B. Hydrazone Analogues: Molecular Modeling, Synthesis, *In- vivo* Anti-Nociceptive Activity and *in-vitro* Antimicrobial Activity. Egypt J Chem. 2019;62(8):1441-50.

52. Singh J, Kumar M, Mansuri R, Sahoo GC, Deep A. Inhibitor designing, virtual screening and docking studies for methyltrans-ferase: a potential target against dengue virus. J Pharm Bioallied Sci. 2016;8(3):188-94.

53. Joseph A, Shah CKS, Kumar SS, Alex AT, Maliyakkal N, Moorkoth S, et al. Synthesis, *in vitro* anticancer and antioxidant activity of thiadiazole substituted thiazolidin-4-ones. Acta Pharm. 2013; 63:397–408.

Table 1

Table 1 is available in the Supplementary Files section.

Figures

Figure 1

Antibacterial evaluation results against Gram positive species.

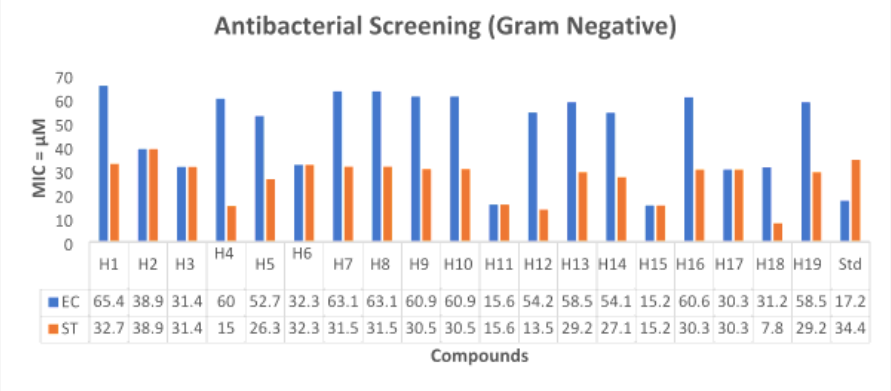

Figure 2

Antibacterial evaluation results against Gram negative species.

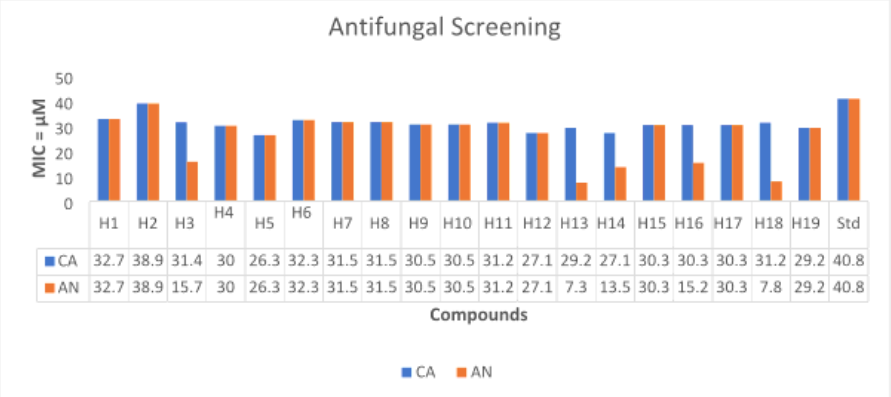

Figure 3

Antifungal evaluation results against fungal species.

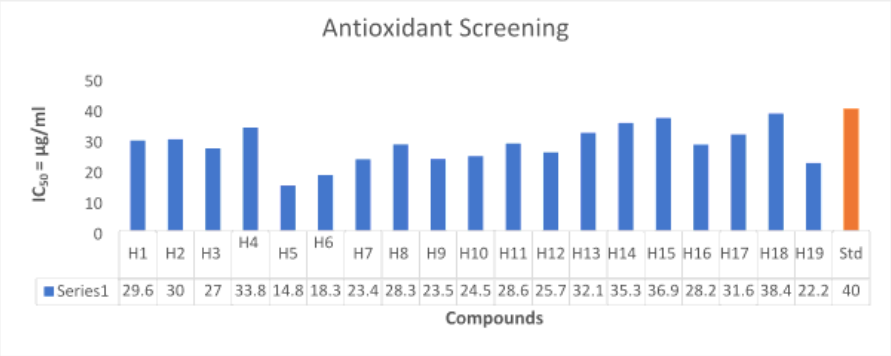

Figure 4

Antioxidant screening of synthesized compounds using ascorbic acid as standard.

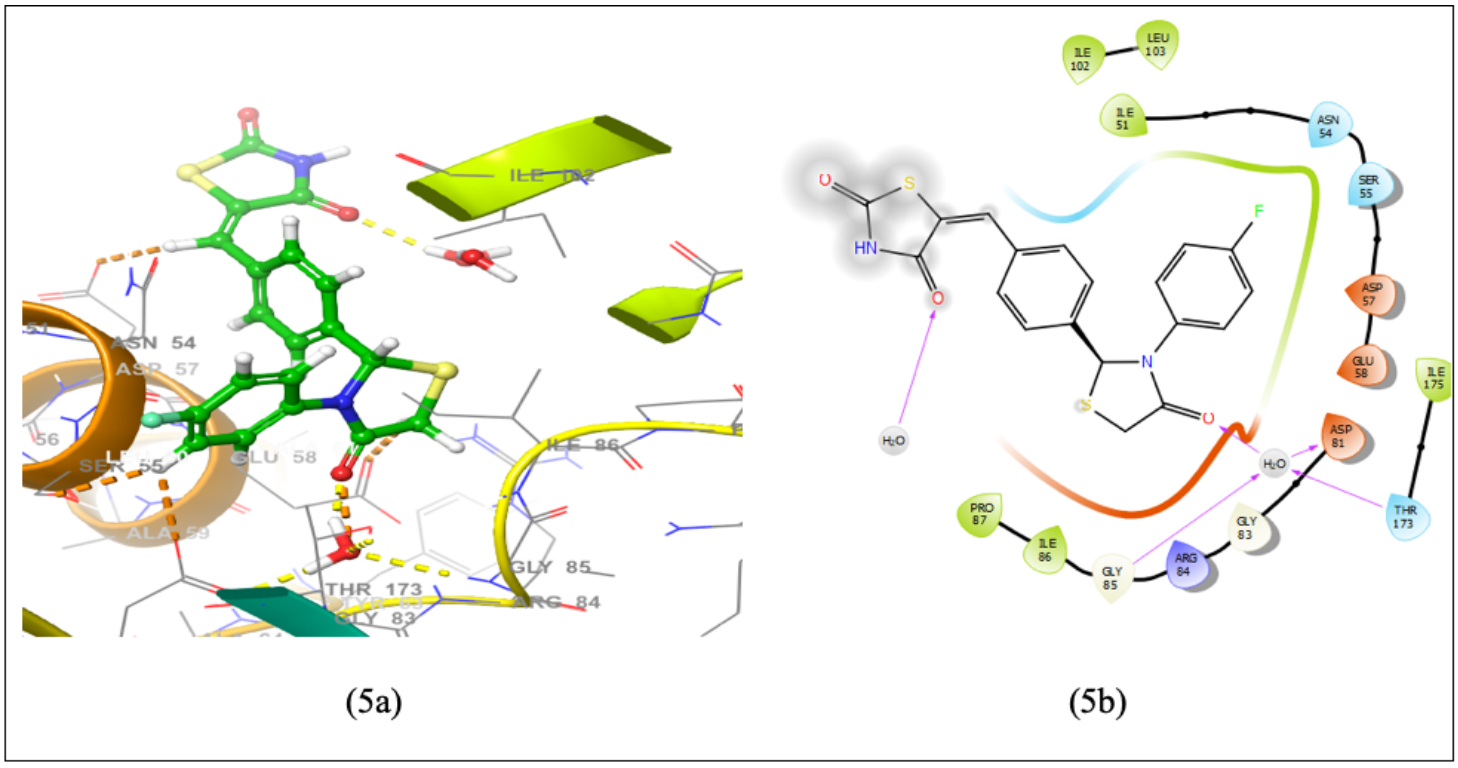

Figure 5

Interaction of compound **H18** and 4-bromo-5-methyl-*N*-[1-(3-nitropyridin-2-yl)piperidin-4-yl]-1H-pyrrole-2-carboxamide within the active pocket of *S. aureus* GyrB ATPase domain protein and interacting amino acid in 3D (5a) and 2D (5b) view.

Figure 6

Interaction of compound **H7** and 4-bromo-5-methyl-*N*-[1-(3-nitropyridin-2-yl)piperidin-4-yl]-1H-pyrrole-2-carboxamide within the active pocket of *S. aureus* GyrB ATPase domain protein and interacting amino acid in 3D (6a) and 2D (6b) view.

Figure 7

Interaction of standard compound ofloxacin and 4-bromo-5-methyl-*N*-[1-(3-nitropyridin-2-yl)piperidin-4-yl]-1H-pyrrole-2-carboxamide within the active pocket of *S. aureus* GyrB ATPase domain protein and interacting amino acid in 3D (7a) and 2D (7b) view

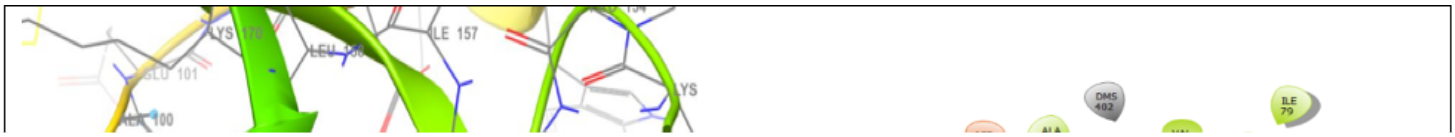

Figure 8

Interaction of compound **H2** and 8-[3-(3-azanyl-2~{H}-indazol-6-yl)-5-chloranyl-pyridin-4-yl]-2,8-diazaspiro[4.5]decan-1-one within the active pocket of cyclin dependent kinase domain protein and interacting amino acid in 3D (8a) and 2D (8b) view

Figure 9

Interaction of compound **H10** and 8-[3-(3-azanyl-2~{H}-indazol-6-yl)-5-chloranyl-pyridin-4-yl]-2,8-diazaspiro[4.5]decan-1-one within the active pocket of cyclin dependent kinase domain protein and interacting amino acid in 3D (9a) and 2D (9b) view

Figure 10

Interaction of standard compound 5-Fluorouracil and 8-[3-(3-azanyl-2~{H}-indazol-6-yl)-5-chloranyl-pyridin-4-yl]-2,8-diazaspiro[4.5]decan-1-one within the active pocket of cyclin dependent kinase domain protein and interacting amino acid in 3D (10a) and 2D (10b) view

Figure 11

Anticancer evaluation results of compounds **H2, H10** and **H11** against DU-145 prostate cancer cell lines.

Figure 12

Structure activity relationship of synthesized compounds

Supplementary Files

This is a list of supplementary files associated with this preprint. Click to download.

- Table1.docx
- floatimage1.jpeg